

Wormhole solutions in generalized Rastall gravity

Naser Sadeghnezhad*

Research Institute for Astronomy and Astrophysics of Maragha (RIAAM), University
of Maragheh, P. O. Box 55136-553, Maragheh, Iran

December 11, 2024

Abstract

In the present work, we seek for static spherically symmetric solutions representing wormhole configurations in generalized Rastall gravity (GRG). In this theory, a varying coupling parameter could act as dark energy (DE) and thus, it can be considered as responsible for the current accelerated expansion of the universe. We consider an anisotropic energy momentum tensor (EMT) as the supporting source for wormhole structure and further assume that there exists a linear relation between radial and tangential pressures and energy density. We therefore obtain two classes of solutions to the field equations of GRG, including the solutions with zero and nonzero redshift functions. For these solutions we find that the matter distribution obeys the physical reasonability conditions, i.e., the flare-out and the weak (WEC) and null (NEC) energy conditions either at the throat and throughout the spacetime. The conditions on physical reasonability of the wormhole solutions put restrictions on model parameters. Hence, in the framework of GRG, asymptotically flat wormhole configurations can be built without the need of exotic matter. Gravitational lensing effects of the obtained solutions are also discussed and it is found that the throat of wormhole can effectively act as a photon sphere near which the light deflection angle takes arbitrarily large values.

1 Introduction

Conceptually, wormholes can be imagined as tube-like geometric structures connecting two separate regions within the same universe or even different universes altogether. The idea of such interesting geometries can originally be traced back to Flamm [1] in 1916 who tried to provide interpretations of the Schwarzschild solution through 2D embedding diagram of Schwarzschild wormhole. In 1935 Einstein and Rosen expanded this concept with the aim of constructing potential models for elementary particles. Their work led to what is now known as the Einstein-Rosen bridge [2]. The term “wormhole” was first introduced by Wheeler in 1957 [3] and further developed by Misner and Wheeler [4, 5]. However, Wheeler wormholes were properly understood as non-traversable since they do not allow a two way communication between two regions of the spacetime by a minimal surface called the wormhole throat [6]. Moreover, it was shown that these wormholes would, in principle, develop some type of singularity [7].

Over the past decades, there has been a huge amount of interest in wormhole physics, the start of which was mainly triggered through the seminal paper by Morris and Thorne [8, 9]. The authors of this article investigated this issue by introducing a static spherically symmetric metric and discussed the physical conditions for a reasonable Lorentzian traversable wormhole that allows a traveler to

*nsadegh@maragheh.ac.ir

experience crossing through the throat of wormhole back and forth both universes. However, the traversability of a wormhole necessitates violation of the null energy condition (NEC) [10] which is a fundamental condition in GR. This condition states that for any null path, the energy density of the matter and fields must be non-negative. In the case of wormholes, the type of matter that would enable such structures to exist is referred to as exotic matter. This exotic matter is characterized by a negative energy density, leading to the peculiar violation of the NEC. Consequently, while the idea of traversable wormholes opens up fascinating possibilities for interstellar travel and connecting distant regions of spacetime, it also challenges our understanding of the fundamental laws of physics and the nature of matter throughout the universe. Although the violation of energy conditions is unacceptable from the common viewpoint of physicists, it has been shown that some effects due to quantum field theory, e.g., Casimir effect can allow for such a violation [11]. Also, negative energy densities which are required to support the wormhole configuration may be produced through gravitational squeezing of the vacuum [12], see also [10, 13] for more details. However, it is generally believed that all classical matter fields respect the standard energy conditions.

Since the work of Morris, Thorne, and Yurtsever [8, 9], researches in the realm of wormhole structures have opened up a new field of study in theoretical physics and several publications have appeared in recent years for example, wormhole geometries constructed by matter fields with exotic EMT [14], phantom or quintom-type energy [15], wormhole geometries with Casimir energy as the supporting matter [9, 16] and wormholes supported by nonminimal interaction between dark matter and dark energy [17], see [18] for a comprehensive review. However, since exotic matter sources violate energy conditions, many attempts have been made so far toward avoiding or at least minimizing the usage of such type of matter fields and instead, modifying GR with the purpose of overcoming the issue of energy conditions within wormhole structures. In this regard, much effort has gone into investigating wormhole solutions in different modified gravity theories such as, Lovelock theories [19], modified gravities with curvature-matter coupling [20], scalar-tensor theories [21], $f(R)$ gravity [22], Einstein-Cartan theory [23, 24], Einstein-Gauss-Bonnet [25] and other theories [26]. The study of wormhole structures has been also done in Rastall gravity [27, 28, 29]. This theory was introduced as a modification to GR by coupling the matter field with spacetime geometry in a non-minimal way [30]. In this setup, Rastall argued that the ordinary conservation law of EMT, i.e., $\nabla_\mu T^{\mu\nu} = 0$ may no longer hold in curved spacetime. The basic motivation for such argument is that the conservation laws have been only tested on the Minkowski spacetime or quasistatic gravitational fields [31]. Another justification for considering modified theories which violate the EMT conservation is to provide a setting to discuss the process of particle production [32]. However, it is known that the conservation of EMT is not obeyed by the particle production process [33]. Thus, Rastall modified this usual conservation law as, $\nabla_\mu T^{\mu\nu} = \lambda \nabla^\nu R$, i.e., the conservation law is proportional to the gradient of the Ricci scalar [30]. Since its advent, Rastall gravitational theory has attracted the attention of many researchers due to its potential applications in cosmological and astrophysical scenarios [34]. This theory is also in good agreement with various observational data and theoretical expectations [35].

Recently, a generalization of Rastall gravity has been introduced in which the Rastall parameter, λ , which is a measure of mutual interaction between matter and geometry, is a varying parameter that depends on spacetime coordinates [31]. It has been argued that in this generalized Rastall gravity (GRG) a running coupling between matter and geometry can play the role of dark energy and hence the current accelerated expansion phase of the universe phase may have been originated from such a dynamic matter-geometry interaction. Moreover, the authors of [31] have shown that in a flat FLRW background, GRG is capable of explaining an inflationary phase even without a matter component. Also, the existence of pre- and post-inflationary solutions in GRG has been reported in [36] and in [37], it has been shown that a varying Rastall parameter could prevent singularity formation at the end of a collapse scenario. Motivated by the above considerations, our aim in the present work is to study wormholes solutions in the framework of GRG. The paper is then organized as follows: In Sec. (2) we briefly review the field equations of GRG. In Subsecs. (2.1) and (2.2) we try to find exact solutions

representing zero as well as non-zero tidal force wormhole structures. Sec. (3) is devoted to gravitational lensing effects and our conclusions are drawn in Sec. (4).

2 Field equations of GRG and Wormhole Solutions

In the framework of original Rastall theory, the Rastall parameter which is a measure of coupling between matter and curvature is a constant [30]. However, this theory cannot remove the need to a mysterious dark energy source in order to describe the accelerated expansion of the universe [38]. In this sense, a simple generalization of Rastall theory has been proposed as

$$\nabla_\mu T^\mu_\nu = \nabla_\nu(\lambda R), \quad (1)$$

in which the Rastall parameter is no longer a constant and can describe the accelerated universe without invoking to a dark energy source [31]. The field equations are as follows

$$G_{\mu\nu} + \kappa \lambda g_{\mu\nu} R = \kappa T_{\mu\nu}, \quad (2)$$

where κ is Rastall gravitational constant [31].

Let us now consider the general static and spherically symmetric line element representing a wormhole spacetime given by

$$ds^2 = -e^{2\Phi(r)} dt^2 + \left(1 - \frac{b(r)}{r}\right)^{-1} dr^2 + r^2 d\Omega^2, \quad (3)$$

where $d\Omega^2 = d\theta^2 + \sin^2\theta d\phi^2$ is the standard line element on a unit two-sphere, $\Phi(r)$ is the redshift function and $b(r)$ is the wormhole shape function. The radial coordinate ranges from r_0 (wormhole's throat) to spatial infinity. At the throat, defined by the condition $r_0 = b(r_0)$, there is a coordinate singularity where the radial metric component g_{rr} diverges, however, the radial proper distance

$$\ell(r) = \pm \int_{r_0}^r \frac{dx}{(1 - b(x)/x)^{1/2}}, \quad (4)$$

is required to be finite. Indeed, at the throat we have $\ell(r_0) = 0$ while, $\ell < 0 (> 0)$ on the left (right) side of the throat. Conditions on redshift and shape functions under which, wormholes are traversable have been discussed completely in [8]. Traversability of the wormhole requires that the spacetime be free of horizons which are defined as the surfaces with $e^{2\Phi(r)} \rightarrow 0$; therefore the redshift function must be finite everywhere. The shape function should satisfy the following conditions [8, 9]:

- (i) $\left(1 - \frac{b(r)}{r}\right) \Big|_{r=r_0} = 0$: This gives the radius of the throat at $r = r_0$.
- (ii) $rb'(r) - b(r) < 0$ for $r > r_0$: This is the fundamental flare-out condition which at the throat reads, $b'(r_0) < 1$.
- (iii) $\frac{b(r)}{r} < 1$ for $r > r_0$: This condition guarantees that the (Lorentzian) metric signature is preserved.
- (iv) $\lim_{r \rightarrow \infty} \frac{b(r)}{r} = 0$: This condition gives the asymptotic flatness of the metric.

Let us now define the time-like and space-like vector fields, respectively as $u^i = [1, 0, 0, 0]$ and $v^i = [0, \sqrt{1 - b(r)/r}, 0, 0]$, so that $u^i u_i = -1$ and $v^j v_j = 1$. The anisotropic EMT of matter source then takes the form

$$T_{ij} = [\rho(r) + p_t(r)]u_i u_j + p_t(r)g_{ij} + [p_r(r) - p_t(r)]v_i v_j, \quad (5)$$

with $\rho(r)$, $p_r(r)$, and $p_t(r)$ being the energy density, radial and tangential pressures, respectively. We therefore obtain the components of field equations (1) and (2) as

$$2r^2\lambda(r)(r-b(r))\Phi'''(r) + 4r \left(r\lambda(r)(r-b(r))\Phi'(r) + \frac{r}{2}\lambda'(r)(r-b(r)) - \frac{3\lambda(r)}{4} \left[rb'(r) - \frac{4}{3}r + \frac{b(r)}{3} \right] \right) \Phi''(r) \\ - r\lambda(r)(r\Phi'(r) + 2)b''(r) + 2r[r(r-b(r))\lambda'(r) - \lambda(r)(rb'(r) - b(r))] \Phi'^2(r) \\ + [-r\lambda'(r)(3b(r) - 4r + rb'(r)) - 2r\lambda(r)b'(r) + \lambda(6b(r) - 4r) + r^3(p_r(r) + \rho(r))] \Phi'(r) \\ - 2rb'(r)\lambda'(r) + 4\lambda(r)b'(r) + r^2[rp_r'(r) + 2p_r(r) - 2p_t(r)] = 0, \quad (6)$$

$$\rho(r) = 2\lambda(r) \left(1 - \frac{b(r)}{r} \right) [\Phi''(r) + \Phi'^2(r)] - \lambda(r) \left[\frac{b'(r)}{r} - \frac{4}{r} + \frac{3b(r)}{r} \right] \Phi'(r) + (1 - 2\kappa\lambda(r)) \frac{b'(r)}{\kappa r^2}, \quad (7)$$

$$p_r(r) = -2\lambda(r) \left(1 - \frac{b(r)}{r} \right) [\Phi''(r) + \Phi'^2(r)] + \left[\frac{\lambda(r)b'(r)}{r} - \frac{4\lambda(r)}{r} \left(1 - \frac{3b(r)}{4r} \right) + \frac{2}{\kappa r} \left(1 - \frac{b(r)}{r} \right) \right] \Phi'(r) \\ + \frac{2\lambda(r)b'(r)}{r^2} - \frac{b(r)}{\kappa r^3}, \quad (8)$$

$$p_t(r) = \frac{1}{2\kappa r^3} \left\{ -4r^2(r-b(r)) \left(\kappa\lambda(r) - \frac{1}{2} \right) [\Phi''(r) + \Phi'^2(r)] + b'(r)(4r\kappa\lambda(r) - r) + b(r) \right. \\ \left. + r\Phi'(r)[rb'(r)(2\kappa\lambda(r) - 1) - 2\kappa\lambda(r)(4r - 3b(r)) + 2r - b(r)] \right\}. \quad (9)$$

The above equations construct a system of four coupled differential equations to be solved for six unknowns $\{\rho(r), p_r(r), p_t(r), \Phi(r), b(r), \lambda(r)\}$. Hence, this system is under-determined and to solve it one needs to specify the functionality of two of the unknowns. We therefore proceed to deal with this task in the next sections and try to find physically reasonable wormholes solutions.

2.1 Solutions with $\Phi(r) = 0$

In this subsection we proceed to find a consistent solution for the above set of differential equations. To this aim we consider a vanishing redshift function along with linear equations (EoS) of state for radial and tangential pressures as, $p_r(r) = w_1\rho(r)$ and $p_t(r) = w_2\rho(r)$ where w_1 and w_2 are constants. We therefore get three differential equations for three unknowns $\rho(r)$, $\lambda(r)$ and $b(r)$. Hence, the resulted three differential equations can be solved simultaneously for the shape function with the solution given by

$$b(r) = r_0 \left[\frac{r}{r_0} \right]^\delta, \quad \rho(r) = \rho_1 r^\eta + \rho_2 \left(\frac{r}{r_0} \right)^\gamma, \quad \delta = -\frac{w_1 + 2w_2 + 3}{w_1 - 2w_2 - 1}, \quad \gamma = \frac{4(w_2 - w_1)}{w_1 - 2w_2 - 1}, \\ \lambda = \frac{w_1 + 2w_2 + 1}{2\kappa(w_1 + 2w_2 + 3)}, \quad \eta = \frac{2(w_2 - w_1)}{w_1}, \\ \rho_1 = \left[\rho_0 r_0^{\frac{2(w_1 - w_2)}{w_1}} + \frac{2r_0^{\frac{-2w_2}{w_1}}}{\kappa(w_1 - 2w_2 - 1)} \right], \quad \rho_2 = -\frac{2}{\kappa(w_1 - 2w_2 - 1)r_0^2} \quad (10)$$

where r_0 is the radius of wormhole throat. The above solution contains two constants of integration that the first one can be found assuming the value of energy density at the throat as $\rho(r_0) = \rho_0$. The spherical surface $r = r_0$ has to satisfy the fundamental condition (i), i.e., $b(r_0) = r_0$. In order to find the remained integration constant we have used this condition at the wormhole throat. The flare-out condition (ii) at the throat leads to the inequality $\delta < 1$ which also satisfies the asymptotic flatness condition (iv). Also for $\delta < 1$, the ratio $b(r)/r$ stays less than unity for $r > r_0$ hence Lorentzian signature is preserved, as required by condition (iii). In the framework of classical GR, the fundamental

flaring-out condition results in the violation of NEC. Such a violation can be surveyed by applying the focusing theorem on a congruence of null rays, defined by a null vector field k^μ , where $k^\mu k_\mu = 0$ [10, 39]. For the EMT presented in Eq. (5) the NEC is given by

$$\rho(r) + p_r(r) \geq 0, \quad \rho(r) + p_t(r) \geq 0. \quad (11)$$

Also, for the sake of physical reliability of the solutions, we require that the wormhole configuration respects the WEC given by the following inequalities

$$\rho(r) \geq 0, \quad \rho(r) + p_r(r) \geq 0, \quad \rho(r) + p_t(r) \geq 0. \quad (12)$$

We note that WEC implies the null form. The fulfillment of the second and third part of the above conditions requires that $w_1 \geq -1$ and $w_2 \geq -1$. Also the energy conditions at the throat take the form

$$\rho(r) \Big|_{r=r_0} = \rho_0 \geq 0, \quad (13)$$

$$\rho(r) + p_r(r) \Big|_{r=r_0} = \rho_0(1 + w_1) \geq 0, \quad (14)$$

$$\rho(r) + p_t(r) \Big|_{r=r_0} = \rho_0(1 + w_2) \geq 0. \quad (15)$$

We note that the asymptotic flatness requires that no matter distribution is present at spatial infinity or $\rho(r \rightarrow \infty) = 0$. This condition leads to $\eta < 0$ and $\gamma < 0$. In order that the energy density remains positive for $r > r_0$ we may consider three possible cases as follows:

1. $\eta < 0 \quad \wedge \quad \gamma < 0 \quad \wedge \quad \rho_1 \geq 0 \quad \wedge \quad \rho_2 \geq 0$,
2. $\eta < 0 \quad \wedge \quad \gamma < 0 \quad \wedge \quad |\eta| > |\gamma| \quad \wedge \quad \rho_1 < 0 \quad \wedge \quad \rho_2 \geq 0 \quad \wedge \quad \rho_1 + \rho_2 \geq 0$,
3. $\eta < 0 \quad \wedge \quad \gamma < 0 \quad \wedge \quad |\eta| < |\gamma| \quad \wedge \quad \rho_1 \geq 0 \quad \wedge \quad \rho_2 < 0 \quad \wedge \quad \rho_1 + \rho_2 \geq 0$,

Considering now the asymptotic flatness, energy conditions at the throat Eqs. (13)-(15), and flare-out condition we arrive at following inequalities for each of the above three conditions (we have set $r_0 = 1$):

$$\begin{aligned} \rho_0 > 0 \wedge \left\{ \left[\kappa \leq -\frac{2}{\rho_0} \wedge 0 < w_1 \leq 1 \wedge -1 \leq w_2 \leq \frac{\kappa\rho_0(w_1 - 1) + 2}{2\kappa\rho_0} \right] \vee \left[\frac{-2}{\rho_0} < \kappa < \frac{-1}{\rho_0} \wedge \right. \right. \\ \left. \left[\left(w_1 = \frac{-\kappa\rho_0 - 2}{\kappa\rho_0} \wedge w_2 = -1 \right) \vee \left(\frac{-\kappa\rho_0 - 2}{\kappa\rho_0} < w_1 \leq 1 \wedge -1 \leq w_2 \leq \frac{\kappa\rho_0(w_1 - 1) + 2}{2\kappa\rho_0} \right) \right] \right] \vee \\ \left. \left(\kappa = -\frac{1}{\rho_0} \wedge w_1 = 1 \wedge w_2 = -1 \right) \right\}, \end{aligned} \quad (16)$$

for condition 1,

$$\begin{aligned} \rho_0 > 0 \wedge \left\{ \left[\kappa \leq -\frac{2}{\rho_0} \wedge 0 < w_1 < -\frac{1}{\kappa\rho_0} \wedge \frac{\kappa\rho_0(w_1 - 1) + 2}{2\kappa\rho_0} < w_2 < -\frac{1}{2}(w_1 + 1) \right] \vee \right. \\ \left[-\frac{2}{\rho_0} < \kappa < -\frac{1}{\rho_0} \wedge \left[\left(0 < w_1 < \frac{-\kappa\rho_0 - 2}{\kappa\rho_0} \wedge -1 \leq w_2 < -\frac{1}{2}(w_1 + 1) \right) \vee \right. \right. \\ \left. \left(w_1 = \frac{-\kappa\rho_0 - 2}{\kappa\rho_0} \wedge -1 < w_2 < -\frac{1}{2}(w_1 + 1) \right) \vee \left(\frac{-\kappa\rho_0 - 2}{\kappa\rho_0} < w_1 < -\frac{1}{\kappa\rho_0} \wedge \right. \right. \\ \left. \left. \frac{\kappa\rho_0(w_1 - 1) + 2}{2\kappa\rho_0} < w_2 < -\frac{1}{2}(w_1 + 1) \right) \right] \right] \vee \left(-\frac{1}{\rho_0} \leq \kappa < 0 \wedge 0 < w_1 < 1 \wedge -1 \leq w_2 < -\frac{1}{2}(w_1 + 1) \right) \right\}, \end{aligned} \quad (17)$$

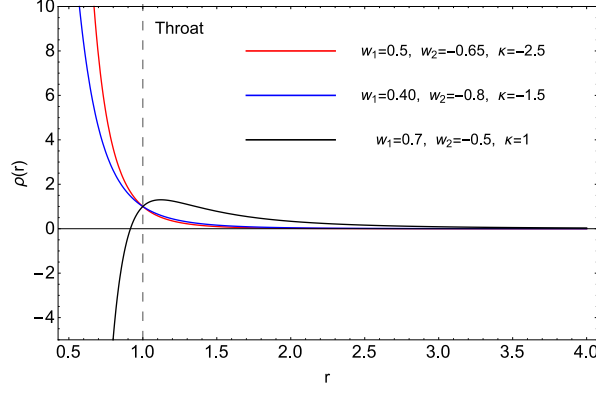


Figure 1: Plot of energy density for $\rho_0 = r_0 = 1$. Right panel: The allowed region for the pair of parameters (w_1, w_2) for $r_0 = \kappa = 1$, $\alpha = 1$, $\beta = -0.3$ (blue region), $\beta = -0.2$ (red region) and $\beta = -0.1$ (gray region).

for condition 2, and

$$\rho_0 \geq 0 \quad \wedge \quad \kappa > 0 \quad \wedge \quad 0 < w_1 \leq 1 \quad \wedge \quad -\frac{1}{2}(w_1 + 1) < w_2 < \frac{w_1 - 1}{2}, \quad (18)$$

for condition 3. Fig. (1) shows the behavior of energy density for different values of EoS parameters according to the above conditions. It is therefore seen that the supporting matter for wormhole configuration obeys the WEC (as long as $-1 \leq w_1 \leq 1$ and $-1 \leq w_2 \leq 1$), either at the throat and throughout the spacetime. A special type of solutions can be found for the case in which the matter distribution obeys the EoS of dark energy in tangential direction, i.e., $w_2 = -1$. For this case $\delta = -1$ and the conditions 1 and 2 are reduced to the following inequalities, respectively

$$\rho_0 > 0 \wedge \left[\left(\kappa \leq -\frac{2}{\rho_0} \wedge 0 < w_1 \leq 1 \right) \vee \left(-\frac{2}{\rho_0} < \kappa < -\frac{1}{\rho_0} \wedge \frac{-\kappa\rho_0 - 2}{\kappa\rho_0} \leq w_1 \leq 1 \right) \vee \left(\kappa = -\frac{1}{\rho_0} \wedge w_1 = 1 \right) \right], \quad (19)$$

$$\rho_0 > 0 \wedge \left[\left(-\frac{2}{\rho_0} < \kappa < -\frac{1}{\rho_0} \wedge 0 < w_1 < \frac{-\kappa\rho_0 - 2}{\kappa\rho_0} \right) \vee \left(-\frac{1}{\rho_0} \leq \kappa < 0 \wedge 0 < w_1 < 1 \right) \right], \quad (20)$$

The third condition does not provide physically reasonable values for the parameters $\{w_1, \rho_0, \kappa\}$. Hence, considering the above two conditions the spacetime metric Eq. (3) is reduced to the following form

$$ds^2 = -dt^2 + \frac{dr^2}{1 - \frac{r_0^2}{r^2}} + r^2 d\Omega^2, \quad (21)$$

which represents the well-known Morris-Thorne spacetime [8].

2.2 Solutions with $\Phi(r) = \frac{1}{2} \ln[\alpha + \beta \left(\frac{r_0}{r}\right)]$

Let us now investigate wormhole solutions with a non-vanishing redshift function. Substituting then for $\Phi(r)$ into Eqs. (6)-(9) together with considering linear EoS in radial and tangential directions we

arrive at a system of coupled differential equations for the three unknowns $\rho(r)$, $\lambda(r)$ and $b(r)$. This system can be solved analytically and the solution is found as

$$\begin{aligned}\rho(r) &= C_1 r^{\frac{4w_2-3w_1+1}{2w_1}} (\alpha r + \beta r_0)^{-\frac{w_1+1}{2w_1}} \\ &+ \frac{C_2(\alpha r + \beta r_0)}{r^2} [2r\alpha(w_1 - 2w_2 - 1) + r_0\beta(3w_1 - 4w_2 - 1)]^{\frac{2w_2-3w_1-1}{w_1-2w_2-1}},\end{aligned}\quad (22)$$

$$\lambda(r) = \frac{2r\alpha(w_1 + 2w_2 + 1) + r_0\beta(w_1 + 4w_2 + 1)}{4\kappa[r\alpha(w_1 + 2w_2 + 3) + 2r_0\beta(w_2 + 1)]}, \quad (23)$$

$$\begin{aligned}b(r) &= \left\{ \frac{\kappa r^3}{4} (\alpha r + \beta r_0) w_1 \left[r\alpha(w_1 - 2w_2 - 1) + \frac{3}{2} \left(w_1 - \frac{4}{3}w_2 - \frac{1}{3} \right) \beta r_0 \right]^2 \rho'(r) \right. \\ &+ \frac{\kappa r^2}{2} \left[\alpha(w_1 - w_2)r + \frac{3}{4} \left(w_1 - \frac{4}{3}w_2 - \frac{1}{3} \right) r_0\beta \right] \left[r\alpha(w_1 - 2w_2 - 1) + \frac{3}{2} \left(w_1 - \frac{4}{3}w_2 - \frac{1}{3} \right) r_0\beta \right]^2 \rho(r) \\ &- r_0\beta \left[\alpha^2(w_1 + 2w_2 + 1)(w_1 - w_2)r^2 + \left[w_1^2 + w_1 \left(\frac{3}{4} + 2w_2 \right) - 4 \left(w_2 + \frac{1}{4} \right)^2 \right] \alpha\beta r r_0 \right. \\ &+ \left. \left. \frac{3}{8}(w_1 + 4w_2 + 1)\beta^2 r_0^2 \left(w_1 - \frac{4}{3}w_2 - \frac{1}{3} \right) \right] \right\} / \left[\alpha \left(\alpha^2(w_1 + 2w_2 + 1)(w_1 - w_2)r^2 \right. \right. \\ &+ \left. \left. \alpha\beta r r_0 \left[w_1^2 + w_1 \left(2w_2 + \frac{3}{4} \right) - 4 \left(w_2 + \frac{1}{4} \right)^2 \right] + \frac{3}{8}(w_1 + 4w_2 + 1)\beta^2 r_0^2 \left(w_1 - \frac{4}{3}w_2 - \frac{1}{3} \right) \right] \right].\end{aligned}\quad (24)$$

where C_1 and C_2 are integration constants. We find the constant C_1 using the value of energy density at the throat, i.e., $\rho(r_0) = \rho_0$ and the constant C_2 , using the condition $b(r_0) = r_0$. A straightforward but lengthy calculation then gives

$$b(r) = \left(r + \frac{\beta}{\alpha} r_0 \right) \left[\frac{A(r)}{A(r_0)} \right]^{1-\epsilon_1} - \frac{\beta}{\alpha} r_0, \quad (25)$$

$$\rho(r) = \frac{1}{\kappa A(r_0) r^2} \left\{ -4(\alpha r + \beta r_0) \left[\frac{A(r_0)}{A(r)} \right]^{\epsilon_1} + \rho_3 \left(\frac{r}{r_0} \right)^{\epsilon_2} \left[\frac{(\alpha + \beta)r_0}{\alpha r + \beta r_0} \right]^{\epsilon_3} \right\}, \quad (26)$$

where

$$\begin{aligned}\epsilon_1 &= \frac{3w_1 - 2w_2 + 1}{w_1 - 2w_2 - 1}, & \epsilon_2 &= \frac{4w_2 + w_1 + 1}{2w_1}, & \epsilon_3 &= \frac{w_1 + 1}{2w_1}, \\ \rho_3 &= 4r_0(\alpha + \beta) + \kappa r_0^2 \rho_0 A(r_0), & A(r) &= 2r\alpha(w_1 - 2w_2 - 1) + r_0\beta(3w_1 - 4w_2 - 1).\end{aligned}\quad (27)$$

It can be easily checked that $b(r_0) = r_0$ and $\rho(r_0) = \rho_0$. Considering the above solution, the following points can be argued:

I . From Eq. (25) the flare-out condition leads to the following inequality at the throat

$$-\frac{2\alpha(2w_2 + w_1 + 3) + \beta(4w_2 + w_1 + 5)}{2\alpha(w_1 - 2w_2 - 1) + \beta(3w_1 - 4w_2 - 1)} < 1. \quad (28)$$

II . From Eqs. (25) and (26) the asymptotic flatness of the solution implies

$$\epsilon_1 > 1 \quad \wedge \quad \epsilon_2 < 0 \quad \wedge \quad \epsilon_3 > 0. \quad (29)$$

III . For the temporal component of metric at spatial infinity we have

$$\lim_{r \rightarrow \infty} e^{2\Phi(r)} = \lim_{r \rightarrow \infty} \left(\alpha + \beta \frac{r_0}{r} \right) = \alpha > 0. \quad (30)$$

IV . The WEC at wormhole throat implies

$$\rho_0 \geq 0, \quad -1 \leq w_1 \leq 1, \quad -1 \leq w_2 \leq 1, \quad (31)$$

V . In order that the energy density remains positive for $r > r_0$, we assume that $\rho_3 > -4r_0(\alpha + \beta)$ and note that the first term in curly brackets of Eq. (26) decays as $1/r^{\epsilon_1-1}$ and the second term as $1/r^{\epsilon_3+|\epsilon_2|}$. Now we may consider the condition $\epsilon_3 + |\epsilon_2| < \epsilon_1 - 1$ so that if at the throat $\rho(r_0) = \rho_0 > 0$, it then remains positive throughout the spacetime.

The left panel in Fig. (2) presents the allowed regions of the pair (w_1, w_2) according to the conditions (I-V) stated above. As we observe, wormhole configurations with a non-vanishing redshift function satisfy the WEC in both directions. The right panel shows the behavior of energy density as a function of radial coordinate for different values of model parameters subject to the conditions (I-V). It is therefore seen that considering the condition IV, the WEC and NEC are satisfied at the throat and throughout the spacetime and thus, there is no need of introducing exotic matter in order to construct the present wormhole solutions. The left panel in Fig. (3) shows the behavior of radial metric component, i.e., $g_{rr} = (1 - b(r)/r)^{-1}$. We observe that g_{rr}^{-1} is positive for $r > r_0$ and thus the metric signature is preserved for radii bigger than the throat radius. We note that the metric is asymptotically flat since, as $r \rightarrow \infty$, both the temporal and radial components of the metric tend to unity. To be a solution of a wormhole, one needs to impose that the throat flares out. This can be seen in the right panel of Fig. (3) as the satisfaction of flare-out condition. In Fig. (4), we have plotted the behavior of Rastall parameter where we observe that this parameter decreases monotonically as one moves away from the wormhole configuration. This behavior may be interpreted in such a way that the effects of a running mutual interaction between matter and geometry, encoded in the variable Rastall coupling parameter, increase in the limit of approach to the wormhole throat and these effects can contribute to constructing wormhole configurations without the need of exotic matter. Moreover, asymptotically the Rastall parameter tends to a constant that the value of which is decided by the EoS parameters of the matter content of the wormhole configuration, see the solution Eq. (10) with vanishing redshift function. We therefore conclude that for the present class of wormhole solutions, the satisfaction of WEC and NEC for a non-vanishing redshift function requires a varying coupling between matter and geometry.

3 Gravitational Lensing

One of the interesting features of a compact object in the universe is its gravitational lensing effects. Wormholes are no exception as lensing effects of these objects can provide a way to search for their observational signatures. In the present section we investigate lensing features of the obtained wormhole solutions. To this aim we need to study the behavior of null geodesics traveling within the wormhole spacetime. The starting point of our study is the following Lagrangian

$$2\mathcal{L} = g_{\mu\nu}\dot{x}^\mu\dot{x}^\nu = -e^{2\Phi(r)}\dot{t}^2 + \left(1 - \frac{b(r)}{r}\right)^{-1} \dot{r}^2 + r^2\dot{\phi}^2, \quad (32)$$

where use has been made of the spacetime metric (3) and an overdot denotes derivative with respect to the curve parameter ζ . Because of the spherical symmetry we consider the equatorial plane $\theta = \pi/2$. The Lagrangian $\mathcal{L}(\dot{x}, x)$ is constant along a geodesic curve, so one can classify the spacetime geodesics as, timelike geodesics (the world lines of freely falling particles) for which $\mathcal{L} < 0$, lightlike ones (light rays) for which $\mathcal{L} = 0$ and spacelike geodesics for which $\mathcal{L} > 0$. Since the Lagrangian (32) does not

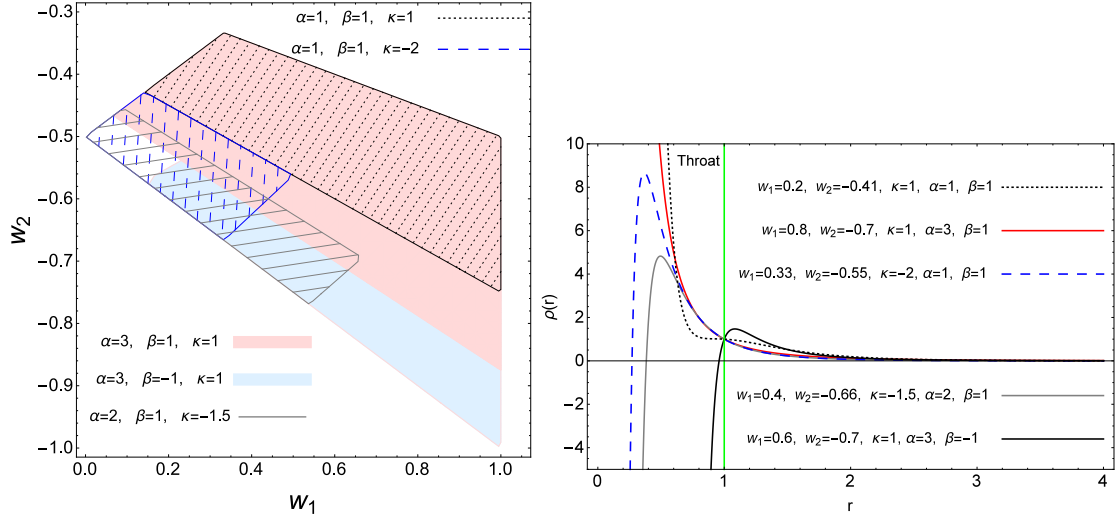


Figure 2: Left panel: The allowed values of EoS parameters for $r_0 = \rho_0 = 1$. Right panel: Behavior of energy density for the allowed values of model parameters chosen from the left panel.

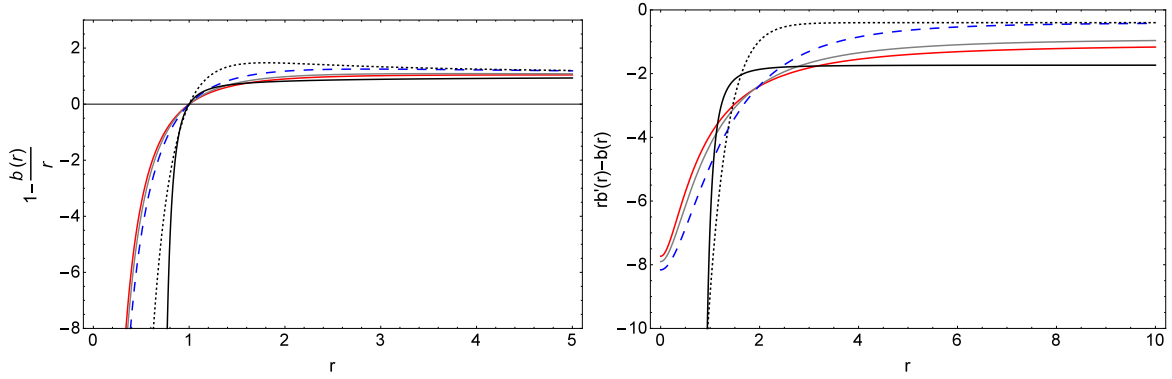


Figure 3: The behavior of inverse of the radial metric component (left panel) and the flare-out condition (right panel) for the same values of model parameters as of the right panel in Fig. (2).

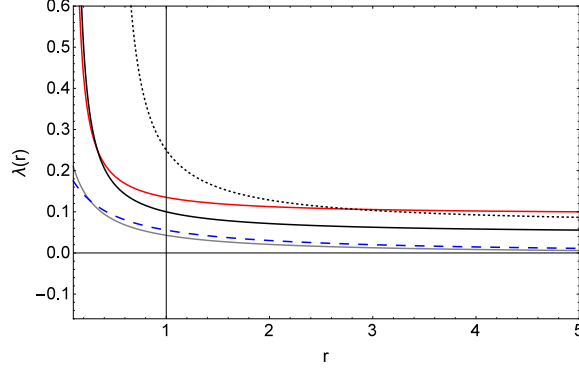


Figure 4: The behavior of Rastall parameter for the same values of model parameters as of the right panel in Fig. (2).

depend on the variables t and ϕ , we have two constants of motion given by

$$\frac{\partial \mathcal{L}}{\partial \dot{t}} = -e^{2\Phi(r)} \dot{t} = -E, \quad (33)$$

$$\frac{\partial \mathcal{L}}{\partial \dot{\phi}} = r^2 \dot{\phi} = L, \quad (34)$$

where E and L are the energy and angular momentum of the light-like particle moving on its orbit, respectively. The condition on null geodesics ($\mathcal{L} = 0$) leaves us with the following equation for photon trajectory

$$\dot{r}^2 + e^{-2\Phi(r)} \left[1 - \frac{b(r)}{r} \right] (V_{\text{eff}}(r) - E^2) = 0, \quad V_{\text{eff}}(r) = \frac{L^2 e^{2\Phi(r)}}{r^2}, \quad (35)$$

where V_{eff} is the effective potential. For a photon coming from a distant source, taking a turn at r_{tp} and escaping then to a faraway observer the deflection angle is given by [40]

$$\theta(r_{\text{tp}}) = 2 \int_{r_{\text{tp}}}^{\infty} \frac{e^{\Phi(r)} dr}{\left[(r^2 - rb(r)) \left(\frac{r^2}{r_{\text{im}}^2} - e^{2\Phi(r)} \right) \right]^{\frac{1}{2}}} - \pi, \quad (36)$$

where $r_{\text{im}} = L/E$ is the impact parameter and the turning point r_{tp} is given by the condition $dr/d\phi = 0$. This condition leads to the following relation between impact parameter and turning point

$$r_{\text{im}} = r_{\text{tp}} e^{-\Phi(r_{\text{tp}})}. \quad (37)$$

Strong gravitational lensing occurs when r_{tp} is close to the location of the photon sphere, i.e., a radius at which light can bend in angles excess of 2π [41]. The conditions for circular photon orbits are given by $\dot{r} = 0$ and $\ddot{r} = 0$ and stable (unstable) photon orbits satisfy the additional condition $\ddot{r} < 0 (> 0)$ [42, 43]. These conditions can be reexpressed in terms of effective potential as

$$V_{\text{eff}}(r) \Big|_{r=r_{\text{ph}}} = E^2, \quad V'_{\text{eff}}(r) \Big|_{r=r_{\text{ph}}} = 0, \quad V''_{\text{eff}}(r) \Big|_{r=r_{\text{ph}}} < 0. \quad (38)$$

where r_{ph} denotes the radius of photon sphere. Therefore, the local maximum points of the effective potential provide unstable photon orbits, while those of local minima give stable ones. The family of unstable photon orbits construct the photon sphere. From Eq. (35) we find that the condition $\dot{r} = 0$

is also satisfied at wormhole throat since $b(r_0) = r_0$. Hence, one may deduce that the throat can play the role of an effective photon sphere when the conditions $\ddot{r} = 0$ and $\ddot{r} > 0$ are fulfilled. In [44], it has been shown that this happens when the following conditions on effective potential are satisfied

$$V_{\text{eff}}(r)\Big|_{r=r_0} = E^2, \quad V'_{\text{eff}}(r)\Big|_{r=r_0} < 0, \quad (39)$$

where use has been made of the flare-out condition $b'(r_0) < 1$. If the photon sphere is situated at the throat then V_{eff} must admit a maximum value at $r = r_0$. To better understand the issue one may switch to radial proper distance given in Eq. (4). Hence, Eq. (35) reads

$$\dot{\ell}^2 e^{2\Phi(r(\ell))} + V_{\text{eff}} = E^2, \quad V_{\text{eff}} = \frac{L^2 e^{2\Phi(r(\ell))}}{r^2(\ell)}. \quad (40)$$

Therefore at the throat, we get the following conditions

$$\begin{aligned} V_{\text{eff}}(r)\Big|_{r=r_0} &= E^2, \quad \frac{dV_{\text{eff}}}{d\ell}\Big|_{\ell=0} = \pm \left[1 - \frac{b(r)}{r}\right]^{\frac{1}{2}} V'_{\text{eff}}(r)\Big|_{r=r_0} = 0, \\ \frac{d^2 V_{\text{eff}}}{d\ell^2} &= \left[1 - \frac{b(r)}{r}\right]^{\frac{1}{2}} V''_{\text{eff}}(r)\Big|_{r=r_0} + \frac{1}{2} \left[\frac{b(r)}{r^2} - \frac{b'(r)}{r}\right] V'_{\text{eff}}(r)\Big|_{r=r_0} = \frac{1 - b'(r_0)}{2r_0} V'_{\text{eff}}(r)\Big|_{r=r_0} < 0, \end{aligned} \quad (41)$$

where we have considered the conditions $b'(r_0) < 1$ and $b(r_0) = r_0$. Now, we proceed to find the behavior of effective potential as a function of radial proper distance. To this aim we have to get the proper distance in terms of radial coordinate through Eq. (4). For zero tidal force solutions Eq. (10), we have

$$\ell(r) = \mp \frac{2r\sqrt{1-r^{1-\delta}}}{(\delta-3)\sqrt{1-r^{\delta-1}}} {}_2F_1\left[\frac{1}{2}, \frac{\delta-3}{2(\delta-1)}, \frac{5-3\delta}{2-2\delta}, r^{1-\delta}\right] \pm \sqrt{\pi} \frac{\Gamma\left[\frac{4-3\delta}{2(1-\delta)}\right]}{\Gamma\left[\frac{2-\delta}{1-\delta}\right]}, \quad (42)$$

where we have set $r_0 = 1$ for simplicity. For $\delta = -1$ which corresponds to Morris-Thorne wormhole [8] the integration can be easily done with the solution $\ell(r) = \pm\sqrt{r^2-1}$. We note that for this case the EoS in tangential direction is that of dark energy and the EoS in radial direction has to obey the conditions given in Eqs. (19) and (20). Then the effective potential is obtained as: $V_{\text{eff}}(\ell) = L^2/(\ell^2 + 1)$. For nonzero redshift solutions Eq. (25), the integral (4) cannot be solved analytically in terms of elementary functions. Hence, we proceed to consider special cases, for example, the case with $\epsilon_1 = 3$ which leads to $w_2 = -1$ and w_1 has to obey the allowed regions given in the left panel of Fig. (2). For this case we choose the model parameters related to the light blue region of this figure, i.e., $\alpha = 3$, $\beta = -1$ and $\kappa = 1$. Then, the integration can be performed with the following result

$$\ell(r) = \pm \frac{3 - 12r + 9r^2 + \sqrt{3}\sqrt{r-1}\sqrt{3r-1} \operatorname{arcsinh}\left[\sqrt{\frac{3}{2}}\sqrt{r-1}\right]}{3\sqrt{3}(2r-1)\sqrt{\frac{3r^2-4r+1}{(1-2r)^2}}}. \quad (43)$$

In the left panel of Fig. (5) we have plotted the effective potential in units of angular momentum squared versus radial proper distance. It is seen that the effective potential admits a maximum at the throat i.e., $\ell = 0$, hence, the throat acts as a photon sphere. The right panel shows the behavior of deflection angle as a function of turning point coordinate radius. We observe that the more the turning point decreases, the more the deflection angle grows. As the turning point tends to the throat radius, the deflection angle increases and diverges at the wormhole throat where an unstable photon sphere is present. In such a situation, the wormhole configuration can produce infinite number of relativistic

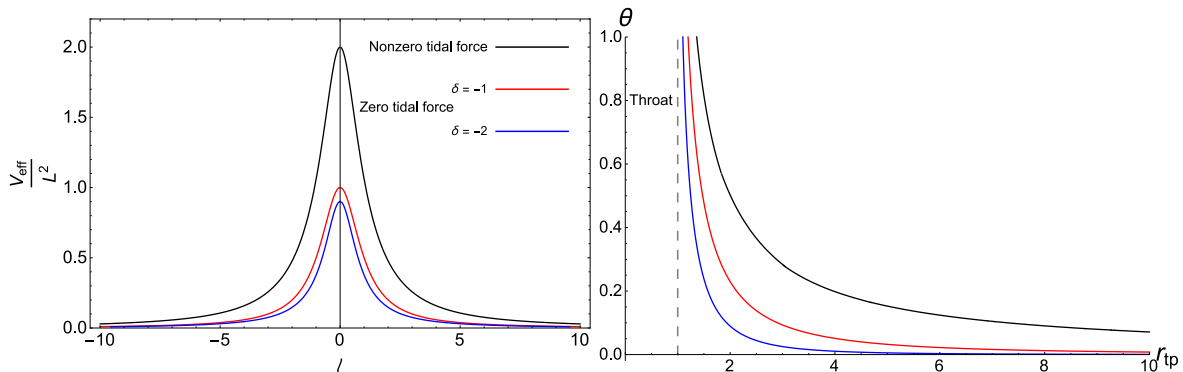


Figure 5: Left panel: The behavior of effective potential against proper radial distance for both zero and nonzero tidal force solutions. For the black curve we have set $\epsilon_1 = 3$, $w_2 = -1$, $\alpha = 3$, $\beta = -1$, $\kappa = 1$ and the EoS in radial obeys the light blue region in the left panel of Fig. (2). Right panel: Behavior of deflection angle against radial coordinate for the same values of model parameters as of the left panel.

images of an appropriately placed source of light. This infinite sequence corresponds to infinitely many light rays whose limit curve asymptotically reaches the unstable photon sphere [42]. In this situation, since the photon sphere coincides with the wormhole throat, such a sphere can be detected utilizing thoroughly and carefully designed modern instruments [43],[45], providing thus, possible observational proofs for the existence of the wormhole.

4 Concluding Remarks

In the framework of GR, the satisfaction of flare-out condition requires the usage of exotic matter which violates the standard energy conditions as respected by normal matter. However, it has been shown that modified gravity theories provide a suitable framework for construction of traversable wormholes without the need of exotic matter or at least minimal usage of such type of matter, see e.g., [23, 24], [18] and [46]. Motivated by these developments, in the present work, we tried to build and study static spherically symmetric wormhole configurations in GRG. We then tried to find exact spacetimes that admit suitable wormhole configurations, considering the field equations of GRG Eqs. (1) and (2). Two classes of exact solutions were obtained and discussed. In the first one, assuming a zero redshift function along with linear EoS between pressure profiles and energy density, we found exact zero tidal force wormhole solutions. We then provided the allowed values of EoS parameters for which the energy conditions as well as conditions on physical reasonability of wormhole solutions are met. The second class of our solutions deals with wormhole structures with nonzero tidal force. For these type of solutions we found that the supporting matter for wormhole geometry satisfies the WEC and NEC, provided that the EoS parameters in radial and tangential directions respect the allowed regions as provided by the left panel of Fig. (2). The study of wormholes in Rastall gravity has been performed by some authors for example, wormhole solutions for traceless fluid in the Rastall background [27], and wormhole solutions in original version of Rastall gravity [28, 29]. These works present examples of wormholes that can exist in Rastall gravity with matter satisfying or violating NEC or even negative energy density at the throat [28]. However, the solutions obtained in the present article respect the WEC and NEC at the throat and throughout the spacetime. This result may be interpreted as the consequences of mutual dynamic interaction between matter and geometry which is encoded in the variable Rastall parameter. Such a dynamic interaction can also provide interesting cosmological as

well as astrophysical models, e.g., successful description of the late time accelerated expansion of the universe [31, 47, 48], evolution of cosmological structures [49], regular cosmological model in the context of Einstein static universe [50], nonsingular collapse scenario [37] and regular black hole solutions [51].

Finally we investigated gravitational lensing effects on the wormhole's surrounding environment and it was found that the effective potential of photons traveling in the wormhole spacetime admits a maximum value at the throat. This result was obtained for a subclass of zero and nonzero redshift solutions and one may be tempted to find more complicated behavior for the effective potential, at or outside of the wormhole throat, see e.g., [52]. This depends on whether the proper radial distance, specifically for non-constant redshift solutions Eq. (25), can be exactly obtained in terms of standard mathematical functions. However, the resultant integral is too complicated to be solved analytically and more advanced mathematical techniques are needed in order to overcome the problem. Consequently, for this subclass of solutions we obtained deflection angle of the incoming beam of light admits positive values and diverges in the limit of approach to the throat. Therefore the wormhole configuration can act as a converging lens with photon sphere located at the throat.

References

- [1] L. Flamm, Phys. Z. **17** 448 (1916); G. W. Gibbons, Gen. Relativ. Gravit. **47** 72 (2015).
- [2] A. Einstein and N. Rosen, Phys. Rev. **48**, 73 (1935);
D. R. Brill and R. W. Lindquist, Phys. Rev. **131**, 471 (1963).
- [3] J. A. Wheeler, Phys. Rev. **97**, 511 (1955).
- [4] C. W. Misner and J. A. Wheeler, Ann. Phys. **2**, 525 (1957);
C. W. Misner, Phys. Rev. **118**, 1110 (1960).
- [5] J. A. Wheeler, Ann. Phys. **2**, 604 (1957);
J. A. Wheeler, Geometrodynamics (Academic, New York, 1962).
- [6] R. W. Fuller and J. A. Wheeler, Phys. Rev. **128**, 919 (1962).
- [7] R. P. Geroch, J. Math. Phys. **8**, 782 (1967).
- [8] M. S. Morris and K. S. Thorne, Am. J. Phys. **56**, 395 (1988).
- [9] M. S. Morris, K. S. Thorne and U. Yurtsever, Phys. Rev. Lett. **61**, 1446 (1988).
- [10] M. Visser, *Lorentzian Wormholes: From Einstein to Hawking* (AIP, Woodbury, USA, 1995);
D. Hochberg and M. Visser, Phys. Rev. D **56**, 4745 (1997).
- [11] H. Epstein, V. Glaser and A. Jaffe, IL Nuovo Cimento, **36**, 1016 (1965).
- [12] D. Hochberg, T. W. Kephart, Phys. Lett. B **268**, 377 (1991).
- [13] G. Klinkhammer, Phys. Rev. D **43**, 2542 (1991).
- [14] S. W. Hawking, Phys. Rev D **46**, 603 (1992);
E. Poisson and M. Visser, Phys. Rev. D **52**, 7318 (1995);
M. Chianese, E. Di Grezia, M. Manfredonia and G. Miele, Eur. Phys. J. Plus **132**, 164 (2017).
- [15] F. S. N. Lobo, Phys. Rev. D **71**, 124022 (2005);
P. K. F. Kuhfittig, Class. Quant. Grav. **23**, 5853 (2006);
F. S. N. Lobo, F. Parsaei and N. Riazi, Phys. Rev. D **87**, 084030 (2013);
Y. Heydarzade, N. Riazi and H. Moradpour, Can. J. Phys. **93**, 1523 (2015).

- [16] R. Garattini, Eur. Phys. J. C **79**, 951 (2019);
 Z. Hassan, S. Ghosh, P. K. Sahoo, V. S. H. Rao, Gen. Relativ. Grav. **55**, 90 (2023);
 O. Sokoliuk, A. Baransky, P. K. Sahoo, Nuc. Phys. B, **930** 115845 (2022);
 S. K. Tripathy, Phys. Dark Univ., **31**, (2021) 100757;
 R. Garattini, Eur. Phys. J. C **81**, 824 (2021);
 P. H. F. Oliveira, G. Alencar, I. C. Jardim, R. R. Landim, Symmetry **15**, 383 (2023); R. Avalos,
 E. Fuenmayor, E. Contreras, Eur. Phys. J. C, **82**, 420 (2022);
 A. H. Ziaie, M. R. Mehdizadeh, Class. Quantum Grav. **41**, 145001 (2024).
- [17] V. Folomeev and V. Dzhunushaliev, Phys. Rev. D **89**, 064002 (2014).
- [18] F. S. N. Lobo, Classical and Quantum Gravity Research, 1-78, (2008), Nova Sci. Pub. ISBN 978-1-60456-366-5, arXiv:0710.4474 [gr-qc].
- [19] G. Dotti, J. Oliva, R. Troncoso, Phys. Rev. D **75**, 024002 (2007);
 H. Maeda, M. Nozawa, Phys. Rev. D **78**, 024005 (2008);
 M. H. Dehghani and Z. Dayyani, Phys. Rev. D **79**, 064010 (2009);
 M. R. Mehdizadeh and F. S. N. Lobo, Phys. Rev. D **93**, 124014 (2016).
- [20] N. M. Garcia and F. S. N. Lobo, Phys. Rev. D **82**, 104018 (2010);
 M. Zubair, S. Waheed and Y. Ahmad, Eur. Phys. J. C **76**, 444 (2016);
 S. K. Tripathy, Phys. Dark Univ., **31**, 100757 (2021);
 A. Dixit, C. Chawla, A. Pradhan, Int. J. Geom. Method Mod. Phys. **18**, 2150064 (2021);
 R. Solanki, Z. Hassan, P. K. Sahoo, Chinese J. Phys., **85** 74 (2023);
 P. H. R. S. Moraes, A. S. Agrawal, B. Mishra, Phys. Lett. B, **855**, 138818 (2024);
 L. V. Jaybhaye, M. Tayde and P. K. Sahoo, Commun. Theor. Phys. **76**, 055402 (2024).
- [21] A. G. Agnese and M. La Camera, Phys. Rev. D **51**, 2011 (1995);
 K. K. Nandi, A. Islam, and J. Evans, Phys. Rev. D **55**, 2497 (1997);
 L. A. Anchordoqui, S. P. Bergliaffa, and D. F. Torres, Phys. Rev. D **55**, 5226 (1997);
 R. Shaikh and S. Kar, Phys. Rev. D **94**, 024011 (2016).
- [22] N. Furey and A. DeBenedictis, Class. Quantum Grav. **22**, 313 (2005);
 F. S. N. Lobo and M. A. Oliveira, Phys. Rev. D **80**, 104012 (2009);
 A. De Benedictis, D. Horvat, Gen. Relat. Gravit. **44**, 2711 (2012);
 M. Sharif and I. Nawazish, Annals of Physics, **389**, 283 (2018);
 R. Radhakrishnan, P. Brown, J. Matulevich, E. Davis, D. Mirfendereski, G. Cleaver, Symmetry, **16**, 1007 (2024).
- [23] K. A. Bronnikov and A. M. Galiakhmetov, Grav. Cosmol. **21**, 283 (2015).
- [24] M. R. Mehdizadeh and A. H. Ziaie, Phys. Rev. D **95**, 064049 (2017);
 Phys. Rev. D **99**, 064033 (2019).
- [25] S. H. Mazharimousavi, M. Halilsoy, and Z. Amirabi, Phys. Rev. D **81**, 104002 (2010);
 P. Kanti, B. Kleihaus and J. Kunz, Phys. Rev. D **85**, 044007 (2012);
 G. Antoniou, A. Bakopoulos, P. Kanti, B. Kleihaus and Jutta Kunz, arXiv:1904.13091 [hep-th].
- [26] R. Shaikh, Phys. Rev. D **92**, 024015 (2015);
 F. Rahaman, N. Paul, A. Banerjee, S. S. De, S. Ray and A. A. Usmani, Eur. Phys. J. C **76**, 246 (2016);
 P. H. R. S. Moraes, P. K. Sahoo, Phys. Rev. D **96**, 044038 (2017);
 M. G. Richarte, I. G. Salako, J. P. Morais Graca, H. Moradpour, and A. ovgun, Phys. Rev. D **96**, 084022 (2017);
 K. Jusufi, N. Sarkar, F. Rahaman, A. Banerjee and S. Hansraj, Eur. Phys. J. C **78** 349 (2018).

- [27] G. Mustafa, M. R. Shahzad, G. Abbas, and T. Xia, Mod. Phys. Lett. A **33** 2050035 (2020).
- [28] H. Moradpour, N. Sadeghnezhad, S. H. Hendi, Can. J. Phys, **95** 1257 (2017).
- [29] S. Halder, S. Bhattacharya, S. Chakraborty, Mod. Phys. Lett. A **34**, 1950095 (2019).
- [30] P. Rastall, Phys. Rev. D **6**, 3357 (1972);
P. Rastall, Can. J. Phys. **54**, 66 (1976).
- [31] H. Moradpour, Y. Heydarzade, F. Darabi and Ines G. Salako, Eur. Phys. J. C **77**, 259 (2017).
- [32] G. W. Gibbons and S. W. Hawking, Phys. Rev. D **15**, 2738 (1977);
N. D. Birrell and P. C. W. Davies, “, *Quantum Fields in Curved Space* (Cambridge University Press, Cambridge, 1982).
- [33] L. Parker, Phys. Rev. D **3**, 346 (1971), [Erratum: Phys. Rev.D **3**, 2546 (1971)].
- [34] H. Moradpour, A. Bonilla, E. M. C. Abreu, and J. A. Neto, Phys. Rev. D **96**, 123504 (2017);
H. Moradpour, Y. Heydarzade, C. Corda, A. H. Ziaie, S. Ghaffari, Mod. Phys. Lett. A, **33**, 1950304 (2019);
F.-F. Yuan and P. Huang, Class. Quant. Grav. **34**, 077001 (2017);
I. P. Lobo, H. Moradpour, J. P. Morais Graca, and I. G. Salako, Int. J. Mod. Phys. D **27**, 1850069 (2018);
R. Kumar, S. G. Ghosh, Eur. Phys. J. C **78**, 750 (2018);
K. Bamba, A. Jawad, S. Rafique, et al., Eur. Phys. J. C **78**, 986 (2018);
H. Moradpour and M. Valipour, Can. J. Phys. **98**, 853 (2020);
S. Halder, S. Bhattacharya, S. Chakraborty, Mod. Phys. Lett. A **34**, 1950095 (2019);
R. Li, J. Wang, Z. Xu and X. Guo, MNRAS, **486**, 2407 (2019);
A. M. Oliveira, H. E. S. Velten, J. C. Fabris, L. Casarini, Phys. Rev. D **92**, 044020 (2015);
S. K. Maurya, F. Tello-Ortiz, Phys. Dark Univ. **29**, 100577 (2020);
X.-C. Cai, Y.-G. Miao, Phys. Rev. D **101**, 104023 (2020).
- [35] F. Darabi, H. Moradpour, I. Licata, et al., Eur. Phys. J. C **78**, 25 (2018).
- [36] D. Das, S. Dutta and S. Chakraborty, Eur. Phys. J. C **78**, 810 (2018).
- [37] A. H. Ziaie, H. Moradpour, M. Mohammadi Sabet, Eur. Phys. J. Plus **136**, 1085 (2021).
- [38] C. E. M. Batista, M. H. Daouda, J. C. Fabris, O. F. Piattella and D. C. Rodrigues, Phys. Rev. D **85**, 084008 (2012).
- [39] F. S. N. Lobo (Editor), “ *Wormholes, Warp Drives and Energy Conditions*,” Springer (2017).
- [40] S. Weinberg, “*Gravitation and cosmology: principles and applications of the general theory of relativity*,” Wiley (1972);
V. Bozza, Gen. Relativ. Gravit. **42**, 2269 (2010);
R. Shaikh, P. Banerjee, S. Paul, T. Sarkar, Phys. Rev. D **99**, 104040 (2019).
- [41] V. Bozza, Phys. Rev. D **66**, 103001 (2002).
- [42] W. Hasse and V. Perlick, Gen. Relativ. Gravit. **34**, 415 (2002).
- [43] V. Perlick, Living Rev. Relativity, **7**, 9 (2004).
- [44] R. Shaikh, P. Banerjee, S. Paul and T. Sarkar, Phys. Lett. B **789**, 270 (2019).

- [45] M. Silvia and R. Esteban, “*Gravitational Lensing And Microlensing*,” World Scientific (2002);
F. Courbin and D. Minniti, (Eds.), “*Gravitational Lensing: An Astrophysical Tool*,” Springer (2008);
M. Kilbinger, Rep. Prog. Phys. **78**, 086901 (2015);
S. Dodelson, “*Gravitational Lensing*,” Cambridge University Press (2017).
- [46] F. S. N. Lobo, M. A. Oliveira, Phys. Rev. D **80**, 104012 (2009);
A. Chanda, S. Dey, B. C. Paul, Gen. Relativ. Gravit. **53**, 78 (2021);
T. Harko, F. S. N. Lobo, M. K. Mak, S. V. Sushkov, Phys. Rev. D **87**, 067504 (2013);
S. Bhattacharya, S. Halder, S. Chakraborty, Mod. Phys. Lett. A **34**, 1950200 (2019).
- [47] H. Shabani, H. Moradpour, A. H. Ziaie, Phys. Dark Univ., **36**, 101047 (2022).
- [48] K. Lin, WL. Qian, Eur. Phys. J. C **80**, 561 (2020).
- [49] A. H. Ziaie, H. Moradpour, H. Shabani, Eur. Phys. J. Plus **135**, 916 (2020).
- [50] H. Shabani, A. H. Ziaie, H. Moradpour, Ann. Phys., **444**, 169058 (2022).
- [51] K. Lin and W.-L. Qian, Chinese Phys. C **43**, 083106 (2019).
- [52] R. Shaikh, P. Banerjee, S. Paul, T. Sarkar, JCAP 07 (2019) 028;
N. Godani, Int. J. Geom. Meth. Mod. Phys. **20**, 2350005 (2023);
N. Godani, G. C. Samanta, Ann. Phys., **429**, 168460 (2021).